

**DEVELOPMENT OF A COLLAGEN-BASED MODEL FOR
TESTING NANOPARTICLE DRUG DELIVERY TO TUMORS**

A Thesis
Presented to
The Academic Faculty

by

Manuela Sushnitha

In Partial Fulfillment
of the Requirements for the Degree
B.S. in Biomedical Engineering with Research Option
in the Wallace H. Coulter School of Biomedical Engineering

Georgia Institute of Technology
May 2016

**DEVELOPMENT OF A COLLAGEN-BASED MODEL FOR
TESTING NANOPARTICLE DRUG DELIVERY TO TUMORS**

Approved by:

Dr. Susan Thomas, Advisor
School of Biomedical Engineering
Georgia Institute of Technology

Dr. James Dixon
School of Biomedical Engineering
Georgia Institute of Technology

Date Approved: 05/03/2016

ACKNOWLEDGEMENTS

I would like to thank Dr.Susan Thomas for providing me with the opportunity to work in her lab and offering her support in the work I did. In addition, I would like to also thank the members of the Thomas lab, especially Alex Schudel, in offering their technical expertise and encouragement. Finally, Andrew Shaw was very helpful in helping me troubleshoot through the imaging process.

TABLE OF CONTENTS

	Page
ACKNOWLEDGEMENTS	vi
LIST OF TABLES	ix
LIST OF FIGURES	x
LIST OF SYMBOLS AND ABBREVIATIONS	xii
SUMMARY	xii
<u>CHAPTER</u>	
1 Introduction	1
2 Literature Review	4
EPR Effect and Nanoparticles	4
Challenges with Current Methods	5
Nanoparticle Drug Testing	6
3 Materials and Methods	8
Collagen Gels: High-Density	8
Collagen Gels: Low-Density	9
Confocal Imaging	10
Diffusion Experiment Setup	12
4 Results	15
Confocal Imaging	15
Diffusion Experiments	18
5 Discussion	20
Confocal Imaging	20
Diffusion Experiments	21

6 Conclusion	23
REFERENCES	24

LIST OF TABLES

	Page
Table 1: Volume of reagents for gels of varying concentrations	9
Table 2: R_h values for dextrans used	14
Table 3: Diffusion coefficient values for dextrans tested	18
Table 4: Literature values for diffusion coefficients	19

LIST OF FIGURES

	Page
Figure 1: Imaging setup using coverslips and glass slides, showing gelled collagen	10
Figure 2: 12-well plate setup for diffusion experiments	13
Figure 3: Confocal images for gels of concentration 5 mg/mL	15
Figure 4: Confocal images for gels of concentration 7 mg/mL	16
Figure 5: Process method for quantification of images	16
Figure 6: Average collagen positive area for the two concentrations of gels	17
Figure 7: Average collagen positive area with respect to gel location in the image	18
Figure 8: Dextran diffusion in collagen gels	19

LIST OF SYMBOLS AND ABBREVIATIONS

EPR	Enhanced Permeability and Retention
NPs	Nanoparticles
kDa	kiloDaltons
MDa	million Daltons

SUMMARY

Cancer continues to take many lives each year and has posed a seemingly insurmountable challenge to scientists around the world. Traditional methods of treatment, including chemotherapy, are ineffective and result in undesirable effects on healthy tissue. As a result, researchers are seeking new methods of targeted therapy that will kill only tumor cells. Stemming from the discovery of the Enhanced Permeability and Retention (EPR) effect and recent advances in nanotechnology, one such method involves the use of nanoparticles as drug carriers into the core tumor tissue by taking advantage of characteristic features of the tumor vasculature. Although this method has shown promise in inducing targeted effects, effective distribution of these particles *in vivo* are inhibited by a host of factors, including the dense collagen matrix that makes up tumors. Furthermore, the failure of animal model study results to translate into positive outcomes in human trials has warranted the need for new testing methods that model the *in vivo* tumor conditions seen in patients. This study aims to address both these issues by developing a basis of experiments that can be utilized for the development of a collagen-based microfluidic device for nanoparticle-based drug delivery testing.

CHAPTER 1

INTRODUCTION

Each year, approximately 8 million individuals around the world die of cancer [1]. Despite the many advancements in technology and medicine in recent decades, traditional methods of treatment, such as surgery and chemotherapy, continue to fail to provide consistent efficacies for treating patients. This motivated the field to develop and test new methods of targeted treatment. The goals of these new techniques are focused on drug delivery to the tumor tissue, ensuring only tumor cells are targeted by the medicine. Emerging discoveries on the architecture of the tumor microenvironment have provided new avenues by which to deliver drugs. Furthermore, recent advancements in nanotechnology have allowed scientists and engineers to begin using a tumor's physical properties as an alternate method of targeted drug delivery.

The foundations for the use of this method of targeted treatment began with the understanding of the enhanced permeability and retention (EPR) effect in tumors. Early research of this physical phenomenon began in the 1980s. In 1986, Matsumura and Maeda found that the poorly-developed tumor vasculature resulted in “leaky” blood vessels [2]. As a result, molecules falling within a specific size range extravasated into the tumor microenvironment. After this initial discovery, nanoparticle-based drug carriers were developed to exploit this phenomenon. Over the course of the next 25 years, researchers have continued to work with these nanoparticles to develop a fine-tuned drug delivery system that targets only tumor cells.

Although a great amount of research has been dedicated to the development of these new drug-carrying particles, scientists have faced many challenges in testing these

molecules for their efficacy *in vivo*. Most studies utilize animal models in which mice are artificially induced to develop tumors and subsequently injected with various concentrations of nanoparticles. Researchers then use *in vivo* imaging and other techniques to measure the effectiveness of the particles in slowing down tumor growth. Although there are variations in the drug delivery system, such as ones in which the particles change size upon reaching the tumor [3] or a communicating system of nanoparticles that locates the tumor and attacks it [4], researchers struggle to reproduce the positive results seen in these mice models during clinical trials in humans. One possible explanation for this discrepancy is the use of mice for validation, models that do not capture all the inherent features of the human body. As a result, a new cohort of researchers is looking into methods of testing that replicate the *in vivo* conditions of solid human tumors. For example, researchers have begun developing a microfluidic device that mimics the fluid flow seen in the tumor vasculature [5]. This device could then be used to test the nanoparticles that other researchers develop.

This study seeks to lay the foundation for the development of a collagen-based model that not only mimics the fiber structure within the tumor microenvironment, but that also can be used to test the diffusion of nanoparticles through this space. This model would be in the form of a microfluidic device that consists of flow channels and an inner core chamber that contains collagen. Flow channel dimensions would be modeled after the blood vessels seen in the tumor microenvironment. Because it is known that tumors have a dense collagen network [6], establishing a method to create collagen gels that are similar to what is seen in tumors will allow for the use of a model that is comparable to the human body. Furthermore, studies have identified that the dense collagen networks

act as one of the primary barriers for nanoparticles [7]. As a result, efficacy of the drugs is significantly decreased due to the low concentration of therapeutic reaching the tumor. By creating this collagen-based model, this study will provide other researchers in this field an alternate method of testing; one that is not only cheaper than animal-based models, but also more accurate in replicating the physiological conditions of the human body.

CHAPTER 2

LITERATURE REVIEW

The search to develop targeted treatment methods for cancer has opened my avenues by which to deliver drugs. One such method takes advantage of the physical properties inherent to the vasculature of tumors as a method of drug delivery. Despite how promising this technique has been to shown to be, more studies are needed to develop a more efficient model that cannot only be used to test this approach, but also ensure it simulates the physiological properties seen in the tumor tissue.

EPR Effect and the Use of Nanoparticles

Early research in this field began with work that sought to understand the underlying properties of the tumor microenvironment. The most significant discovery that emerged from this focus area was the identification of the EPR (Enhanced Permeability and Retention) effect. Research found that certain proteins accumulated in the tumor tissue space. This was in large part due to the vasculature of most solid tumors, largely comprised of leaky blood vessels [2]. Further research found that only molecules of certain sizes possessed the ability to extravasate into the tumor microenvironment [8]. As a result, these molecules accumulate in higher concentrations. This special form of accumulation posed the possibility of its use for targeted drug delivery. Therefore, these findings lead researchers to develop new technology that could take advantage of this research.

With the identification of the EPR effect, researchers began to see the advantageous use of this physiological phenomenon for targeted drug delivery. Because of advances in nanotechnology, scientists began to develop drug carriers that fell within

the given size range dictated by the findings of the EPR theory. These new molecules came in many shapes and forms. Some were hydrogel particles, liposomes or even carbon nanotubes [9]. Studies using this wide variety of molecules showed that different particles could be tuned to have specific properties. However, researchers began to face a host of challenges in the use of these nanoparticles (NPs).

Challenges with Current Methods

As more researchers began utilizing nanoparticles as a means of inhibiting tumor growth, they began to face some challenges in using this developing technology. One of the most common problems faced by scientists was in ensuring proper targeting of these molecules and enhancing deeper tissue penetration. Initially, most individuals were injecting these particles directly into the bloodstream, with the hopes that a reasonable proportion of these NPs would reach the tumor microenvironment due to the size-selectivity of the EPR effect [8]. However, researchers were seeing that a low concentration of these particles was reaching the tumor. Furthermore, even if the molecules did reach the tumor, the NPs were unable to penetrate deeply into the tumor tissue. Studies attempted to circumvent these problems by developing nanoparticle systems that increased the likelihood of these molecules reaching the tumor. For example, particles were created to shrink in size upon entering the tumor microenvironment. This structural change was triggered by proteins specific to the tumor tissue [3]. Others used the knowledge of lower pH in tumors to create molecules that were pH-sensitive. Once the NPs entered the tumor and sensed the change in pH, they shrunk to an appropriate size that would allow for their uptake into the tumor vasculature [10]. Although these studies showed the potential of using these methods of drug delivery, they were still

unable to ensure deep penetration into the tumor space, an area when left untreated has precludes complete elimination of tumor cells.

One key aspect that many of these studies failed to address is the tissue architecture of the tumor environment. Many of these studies did not account for the physical barriers for NP movement inside the tumor. One of the major obstacles that the NPs face in reaching the tumor microenvironment is the dense collagen that makes up the tumor tissue [6]. It is believed that the collagen hinders the diffusion of the nanoparticles inside the body [7]. Despite these findings that highlight the obstructive role of collagen, few studies have looked into understanding how the collagen affects the diffusion of NPs.

Nanoparticle Drug Testing

While testing nanoparticles as drug carries for attacking tumors has shown to be promising, researchers also face the challenge of appropriate methods of testing. Currently, validation of these emerging techniques are conducted in murine models. However, doubts on the effectiveness of using this method of testing have been raised as a result of the failure of these technologies to replicate the positive results seen in mice when carried to human clinical trials. Researchers have begun to point out that xenograft models fail to predict human outcomes because of the “largely unknown factors of extrapolation” [5]. Therefore, this warrants the need for the development of new models that mimic that the physiological conditions seen in the human body. A few recent studies have worked on developing organs on a chip. Among these studies, some researchers have focused their efforts on developing a “tumor on a chip” [5]. This process involves the development of a microfluidic device that comprises of components that are similar to those that make up the tumor microenvironment. For example, it includes

specific channels similar to the lymphatic vessels or the blood vessels that feed into the core of the chip, which models the tumor. This device can then be used to test diffusion of nanoparticles under different conditions. A key feature of the tumor component involves the use of collagen. Although the researchers attempted to mimic the collagen network found in tumors *in vivo*, more knowledge is needed in developing an accurate collagen component.

This study aims to address this challenge associated with the use of NPs by developing a collagen-based model that will provide for an effective method of testing. Because it is known that the collagen network found in tumors obstructs the movement of these particles in this microenvironment, a smaller concentration of the molecules reaches the tumor. As a result, the efficacy of the drug is reduced. This study will develop a collagen model that is based on the physical properties of the collagen network in tumor tissues, specifically through the development of a microfluidic device. This device could then be used to study the diffusion of NPs through the fibers and, as a result, provide a better understanding on how the collagen affects the movement of particles. By developing a collagen model that mimics the tumor environment found inside the body, this study will provide not only a method for testing but also gather knowledge that could be used for the future development of a microfluidic device that simulates *in vivo* conditions.

CHAPTER 3

MATERIALS AND METHODS

Two protocols were established for the creation of the collagen gels. One protocol was used for making gels of higher density (i.e. concentration ≥ 3 mg/mL) and other protocol for gels of lower density (i.e. concentration ≤ 3 mg/mL). Having these two distinct protocols allowed for greater flexibility in the types of gels for subsequent experiments.

Collagen Gels: High-Density

Materials

- High-density Rat-tail, Collagen, Type I solution (Concentration = 8.6 mg/ml)
- 0.17M EDTA
- 0.1M NaOH
- Bucket of ice
- Tube of sufficient volume
- Ultrapure H₂O

Method

- 1) Placed collagen rat tail solution, 10x PBS (+/+), ultrapure H₂O, 0.1M NaOH and 0.17 EDTA on ice for 10 minutes
- 2) Added 141.78 μ L of collagen rat tail solution to a tube of sufficient volume.
- 3) Added 19.5 μ L of 0.17M EDTA
- 4) Added 3.8 μ L of 0.1M NaOH
- 5) Added appropriate amount of H₂O needed for concentration of gel required
- 6) Swirled tube to mix. Vortexed tube for 10 seconds
- 7) Incubated for at least 24 hours at 37°C and 5% CO₂

Gels of 3 different concentrations (3 mg/mL, 5mg/mL and 7 mg/mL) were made. Table 1 shows the reagents used to make these concentrations of gels.

3 mg/mL	5mg/mL	7 mg/mL
141.78 μ L of collagen stock	141.78 μ L of collagen stock	141.78 μ L of collagen stock
19.5 μ L of 0.17M EDTA	19.5 μ L of 0.17M EDTA	19.5 μ L of 0.17M EDTA
3.8 μ L of 0.1M NaOH	3.8 μ L of 0.1M NaOH	3.8 μ L of 0.1M NaOH
241.3 μ L of H ₂ O	78.8 μ L of H ₂ O	No water

Table 1: Volume of reagents needed for various concentrations of gels

Collagen Gels: Low-Density

Materials

- Rat-tail, Collagen, Type I solution (Concentration = 3 mg/ml)
- 10x PBS (+/+)
- 0.1M NaOH
- Bucket of ice
- Tube of sufficient volume
- pH strips
- Ultrapure H₂O

Method

- 8) Placed collagen rat tail solution, 10x PBS (+/+), ultrapure H₂O and 0.1M NaOH on ice for 10 minutes
- 9) Added starting volume of collagen rat tail solution to a tube of sufficient volume.
- 10) Added a volume of PBS that is equal to 1/9th of the starting volume of the collagen solution.
- 11) Swirled tube to mix. (**NOTE: DID NOT VORTEX**)
- 12) Used 0.1M NaOH and pH strips to bring collagen gels solution to a final pH of ~7.4.
 - a. Swirled tube to mix solution after each addition of NaOH. Leave solution in ice during this process
- 13) Determined the final concentration of the collagen gel solution

- a. **NOTE:** Final concentration was at least 1.5 mg/mL.
- b. If final concentration needed to be adjusted, required volume of ultrapure H₂O was added.

14) Pipetted gel solution into a 12-well plate. Incubate for 1hr at 37°C, 5% CO₂

Confocal Imaging

2-photon imaging was used to obtain images of the fibers in the collagen. This imaging step served two purposes: 1) Confirm that the gels were indeed gelling in the appropriate manner 2) Provide visual insight into the fiber network of the collagen gels made.

Slide Setup

Following the protocol described earlier, collagen gel solution of high-density was made. About 15µL of the collagen solution was pipetted onto the coverslips used for glass slides, ensuring the gel stayed round in shape. After “spotting” a coverslip with a drop of collagen, slips were placed onto a glass slide (collagen “spot” facing up) and then incubated for at least 24 hours. Once the coverslips and slides were removed from the incubator, the coverslip (gel side down) was flipped over onto the slide. The coverslips were then taped into place on the slide. Figure 1 shows this final setup.

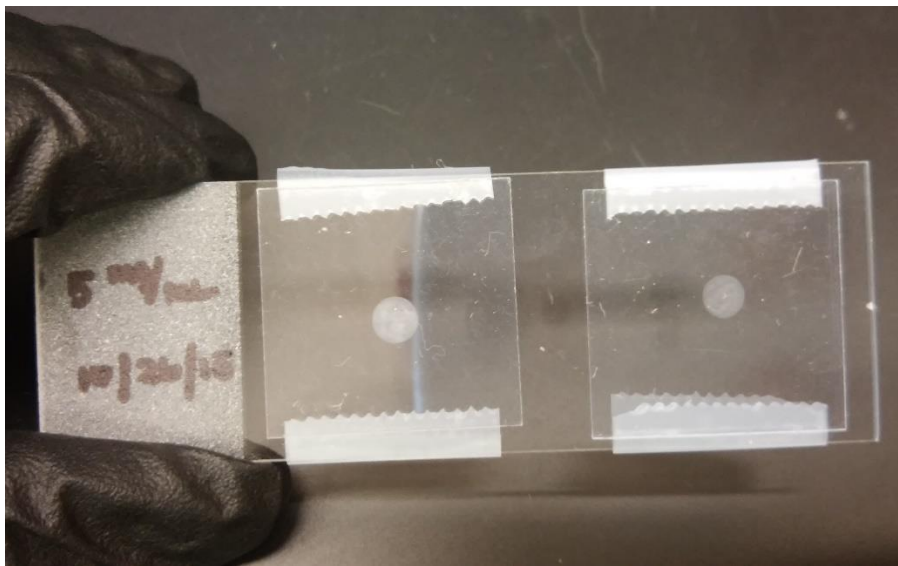


Figure 1: Imaging setup using coverslips and glass slides, showing gelled collagen

Image Acquisition

The following list outlines the settings used on the confocal microscope

- Using the 20x objective, brightfield was used to locate the gel location on the slide
- Emission region of 371-501 nanometers was used
- Laser path consisted of the 800 nanometer laser with plate on top and MBS-690+ filter below
- After switching to live imaging, adjusted the following properties
 - Laser intensity: Between 2-4%
 - Pinhole: Always set to the maximum
 - Master Gain: Ranged from 690-750
 - Number: Did an average of 4 scans
 - Zoom: This was only adjusted when a zoomed-in section of the whole/original image was desired

Quantification of Images

Fiber formation in these images were quantified using ImageJ software. This process involved converting the image files to binary forms (i.e. black and white). Black pixel values were associated with fibers in the gel, while the white values represented the background. These values were then used to calculate the percent of the image area what was collagen positive using the formula below.

$$\text{Collagen positive area (\%)} = \frac{\text{areas with fibers}}{\text{entire image area}} = \frac{\text{number of black pixels}}{\text{total number of pixels}}$$

Comparisons were made between gels of different concentrations and images taken at different locations of the gel on the slide (center vs. outer). In order to make proper comparisons between images, care was to taken ensure all image sizes were the same. A total of 30 images, with 15 images for each concentration, were analyzed using this method.

Diffusion Experiment Setup

A simple diffusion experiment was setup to measure the movement of dextrans in the collagen gels created.

Determining Volume of Dextrans Needed

Before adding dextrans to the gels, the volume of each dextran to be added to the collagen gel solution had to be determined. To test these various volumes, different volumes of each size dextran – 3kDa Texas Red, 10kDa Texas Red, 70kDa Texas Red, and 2M Da Tritc – to 1 mL of 10x (+/+) PBS in a 6-well plate. Fluorescence in each well was then measured using the plate reader, ensuring that there was no overflow and the values fell within a sufficient range that could be read even when the dextrans are added to the collagen gels. After several experiments of using the dextrans in PBS, it was determined to proceed experimentation using only the 3kDa, 70kDa, and 2M Da in a ratio of 1:2.5:5, respectively.

Well Plate Setup

Collagen gels were made according to the low-density collagen protocol described earlier. Final collagen concentration was kept around 1.5 mg/mL (~0.27% w/v solution). However, before pipetting the original collagen solution into the well-plate, the final volume of collagen solution was separated into 3-1.5 mL tubes and an appropriate amount of dextran for a single tube (i.e. Tube 1 contained just the 3kDa dextran and collagen solution, Tube 2 contained just the 70kDa dextran and collagen solution and etc.) was added. Each tube was then mixed well by swirling and each dextran+collagen solution was added to the 12-well plate (Figure 2). The gel solution was pipetted in the bottom “corner” of the well and allowed to gel for 1hr at 37°C and 5% CO₂. The plate was incubated at an angle to ensure the gels remained in the “corner”. After gelation, 1mL of 1x (+/+) PBS was added to all 9 wells. The last row of wells, which served as the control, had the associated volume of dextran added to the 1mL of PBS.

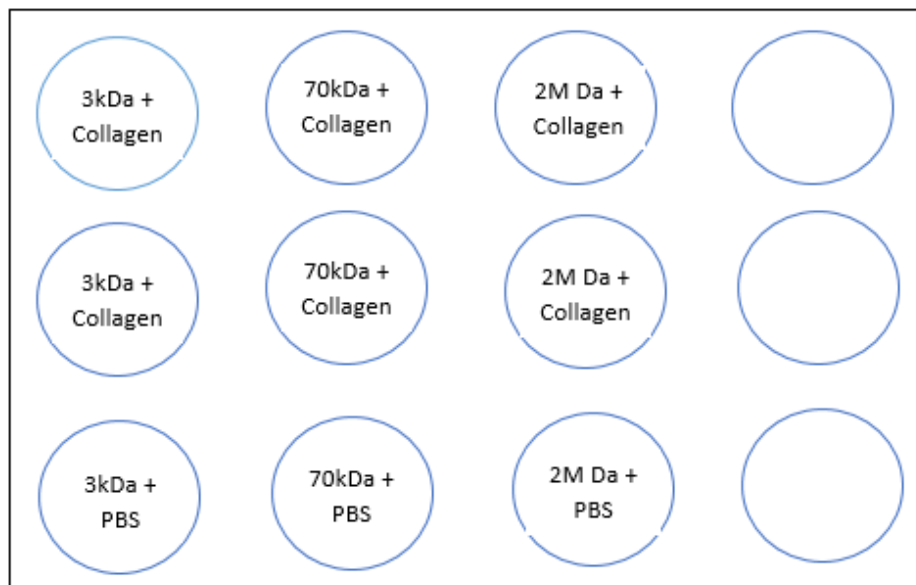


Figure 2: 12-well plate setup for diffusion experiments

Plate Reader Setup

The 12-well plate was then setup to run on the plate reader for a period of 18-21 hours. This setup involved doing a 9x9 area scan of each well at the respective excitation/emission values for each dextran. Both the Texas Red dextrans had excitation/emission values of 595/615, while the Tric dextran had values of 555/585. The fluorescence was measured in the area scans and served as a measure of the diffusion over time. The data collected from the plate reader was analyzed in Excel by plotting the standard deviations of the fluorescence values over time. Because doublets were used for each dextran, the average of the two readings was used when calculating the standard deviations. The final values for each dextran were normalized against the first reading and plotted as a graph.

Diffusion Coefficients

In order to validate the outcome of the diffusion experiments, the diffusion coefficients of each dextran molecule were calculated and compared to literature values found in a previous study. Calculations were made using the following formula from previous work done with collagen gels by Ramanujan et al [11]:

$$D_0 = \frac{k_B T}{6\pi\mu R_h}$$

Here k_B = the Boltzman's constant, T = temperature in Kelvin, μ = viscosity of liquid medium and R_h = the hydrodynamic radius of each dextran.

The use of this formula requires the assumption that the molecule maintains a spherical configuration and the viscosity used was that of PBS. Hydrodynamic radii for each dextran are shown in Table 2.

Molecule	Radii (nm)
3 kDa Texas Red	1.25 ^[12]
70 kDa Texas Red	5.5 ^[12]
2 MDa Tritc	27 ^[13]

Table 2: R_h values for dextrans used

The use of these values allowed for a reasonable expectation for the diffusion experiment that was backed by theoretical models.

CHAPTER 4

RESULTS

Confocal Imaging

Image Acquisition

Images of the collagen gels made were taken using the confocal microscope. Collagen fibers in the gels were most visible in the gels of concentrations 5 mg/mL and 7 mg/mL (Figure 3 and Figure 4). Despite multiple attempts, clear images of the fibers could not be obtained for gels made with concentrations lower than 5 mg/mL. The white portions of the image indicate the fibers present in the gel.

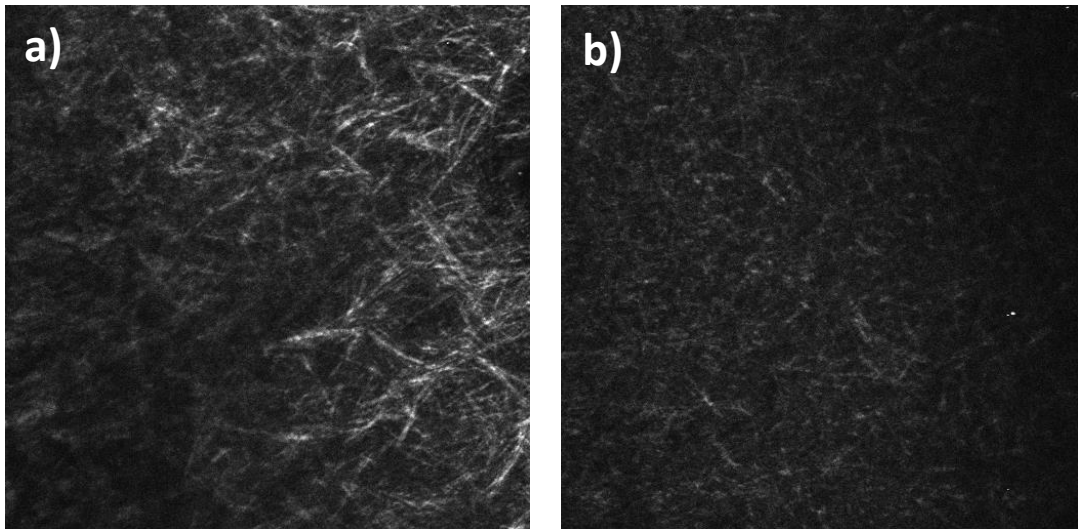


Figure 3: Confocal images for gels of concentration 5 mg/mL with a) being an image taken at the center of the gel and b) taken near the outer edges of the gel

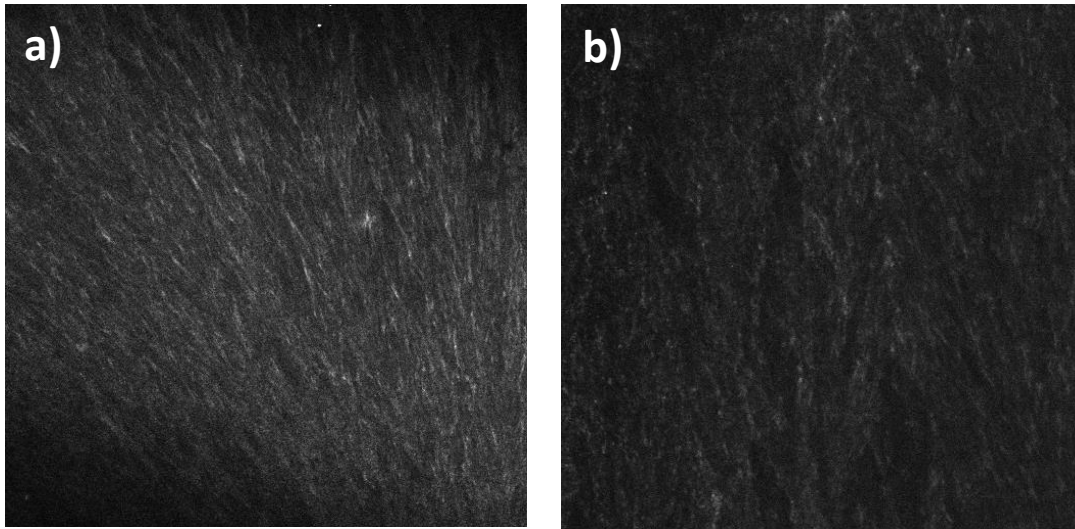


Figure 4: Confocal images for gels of concentration 7 mg/mL a) being an image taken at the center of the gel and b) taken near the outer edges of the gel

Quantification of Images

Fiber formation in the images were quantified using the method outlined previously. Figure 5 shows the process method for a sample image.

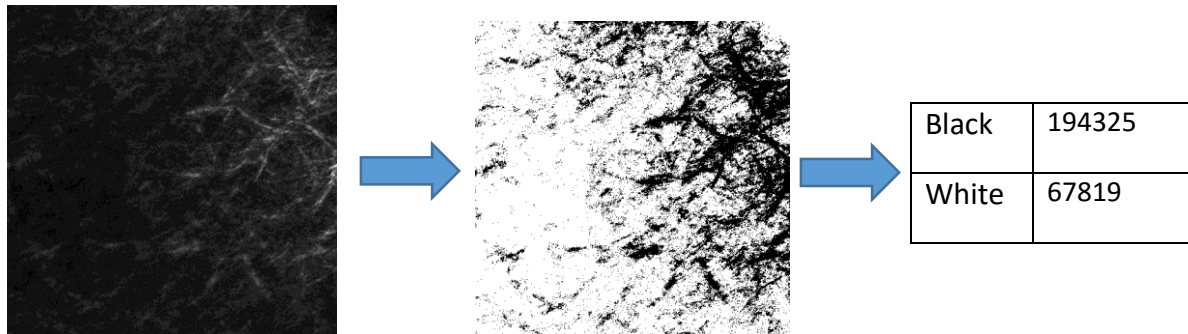


Figure 5: Process method for quantification of images

After quantification of the images, average values of collagen positive areas were determined. Figure 6 demonstrates the average percent of collagen positive areas with respect to concentration.

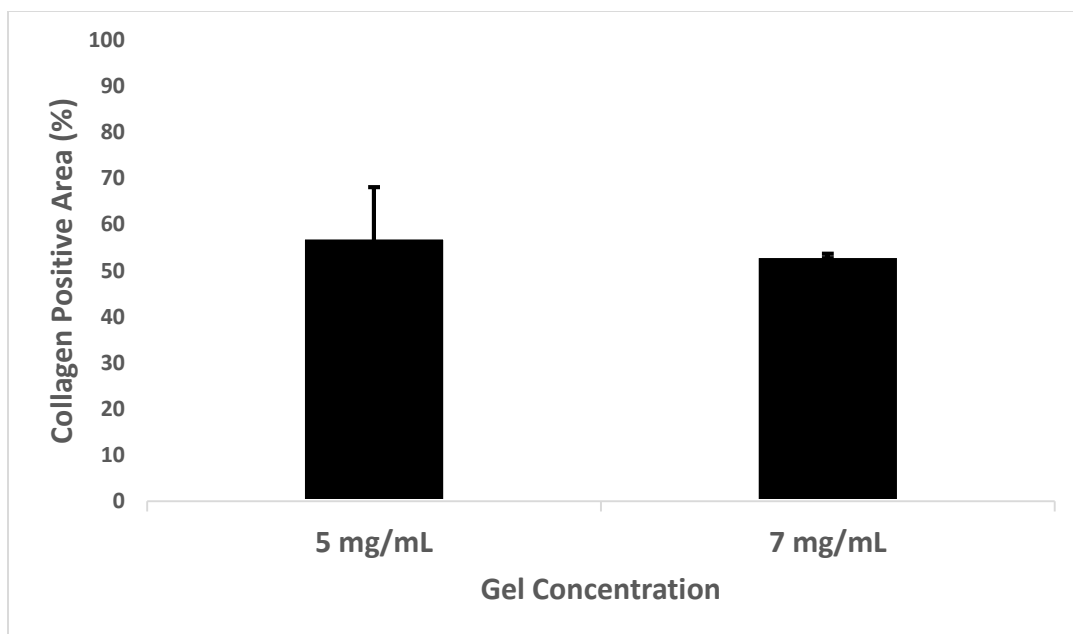
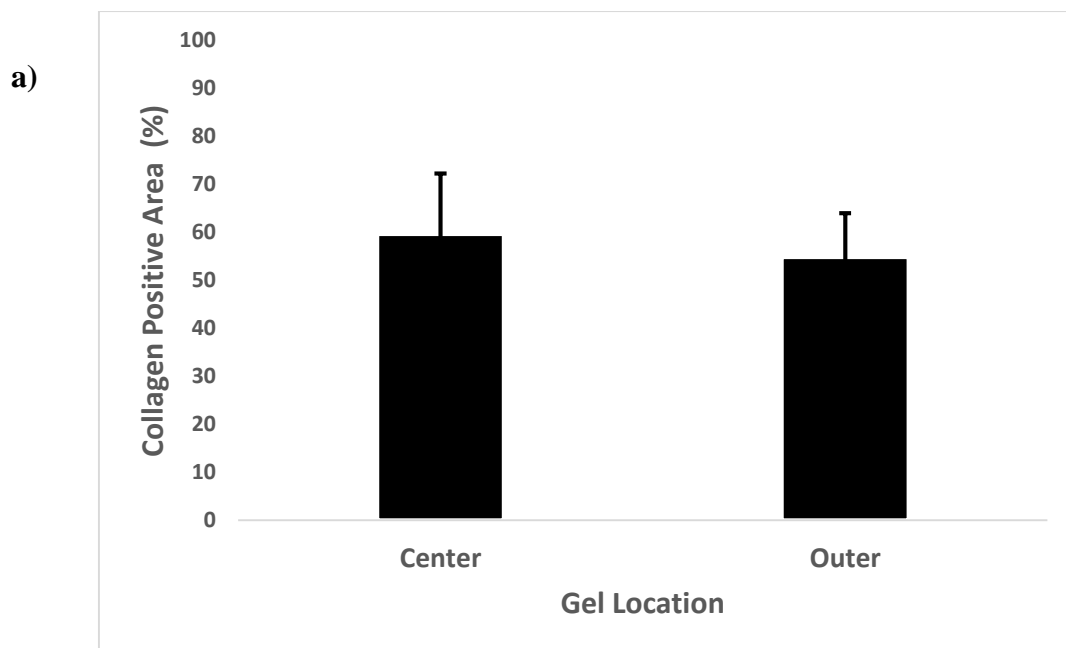


Figure 6: Average collagen positive area for the two concentrations of collagen gels

For each concentration of gel imaged, the percentage of collagen positive areas with respect to position was also determined. Figure 7 shows these results below.



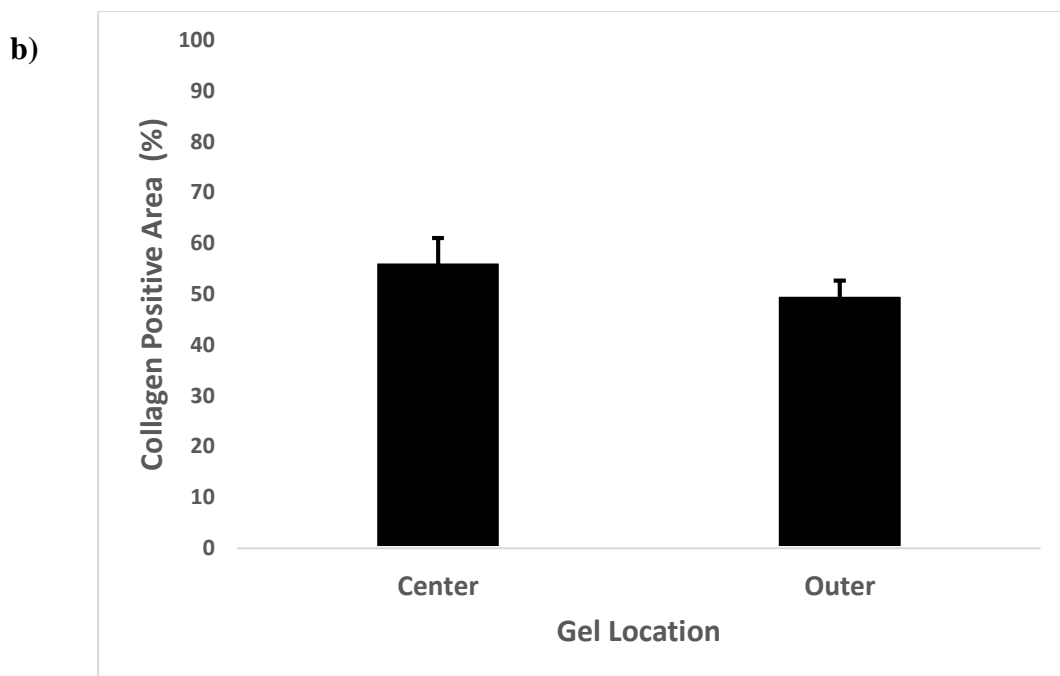


Figure 7: Average collagen positive area with respect to gel location in the image a) 5 mg/mL concentration b) 7 mg/mL concentration

Diffusion Experiment

The calculated diffusion coefficients are shown in the Table 3. As expected, the D_0 values decreased with increasing size of molecule.

Molecule	D_0 (m^2/s)
3 kDa Texas Red	$1.679 * 10^{-10}$
70 kDa Texas Red	$3.817 * 10^{-11}$
2 MDa Tritc	$7.774 * 10^{-12}$

Table 3: Diffusion coefficient values for dextrans tested

These calculated values were then compared to literature values found in previous studies (Table 4). This provided further support for the expected outcome in the diffusion experiment. These values were based on FRAP experiments conducted on 1% w/v solution collagen gels [11].

Molecule	D_0 (m ² /s)
3 kDa Texas Red	$3 * 10^{-8}$
70 kDa Texas Red	$7.8 * 10^{-9}$
2 MDa Tritc	$7.5 * 10^{-10}$

Table 4: Literature values for diffusion coefficients ^[11]

Both these sets of values indicated that diffusion would decrease with increasing size of molecules. As a result, it was expected that the diffusion experiment on the collagen gels created would demonstrate a similar trend. Specifically, the 3kDa would diffuse much faster than the larger 2 MDa dextran.

After the diffusion experiment was conducted, standard deviation values were calculated from the fluorescence readings obtained from the plate reader. These values were then normalized for each dextran and plotted as a function of time (Fig 8). This allowed for measurement of the overall distribution of the dextrans in the well. As a result, these normalized standard deviation values are expected to decrease over time as the dextrans move from being concentrated within the gel alone to being more evenly distributed throughout the well.

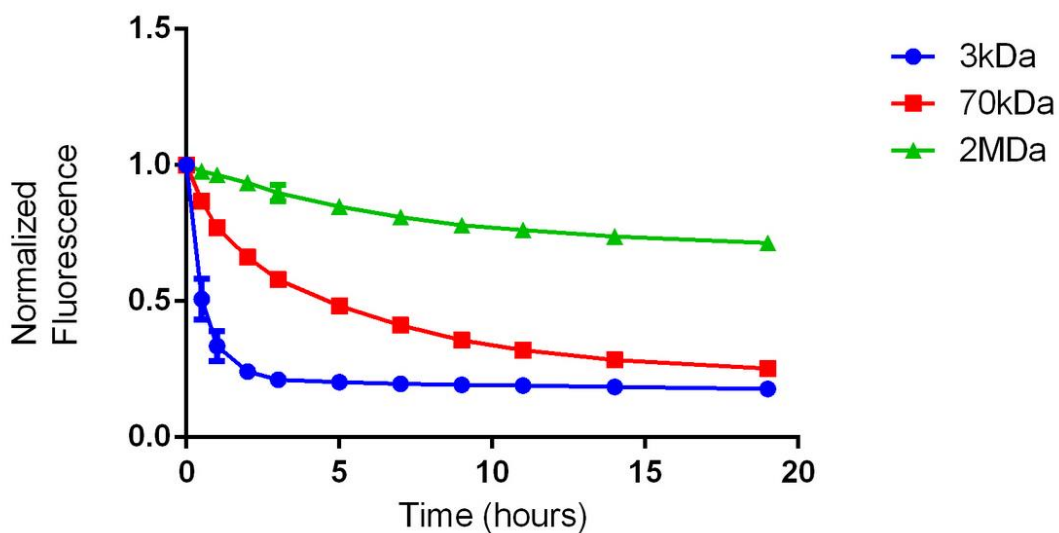


Figure 8: Dextran diffusion in collagen gels

CHAPTER 5

DISCUSSION

Confocal Imaging

The images obtained from the confocal microscope allowed for deeper visualization for the fiber formation in the collagen gels. Some general patterns were seen after analyzing these images further.

Concentration of Gels:

The images shown here were from gels of concentrations 5 mg/mL and 7 mg/mL. This was primarily due to the fact that these gels were the easiest to image. Gain values did not exceed 725, required laser intensity (2-2.5%), and little background noise was seen in these images. Furthermore, a consistent set of property values could be used to image these gels, even between experiments and different batches of gels. In contrast, it was much more difficult to image the 3 mg/mL collagen gels. Despite multiple attempts, the fibers in gels of this concentration were not visible and there was a significant amount of noise when acquiring these images.

Fiber Structure:

As the images shown indicate, the fibers in the collagen gels could be seen using this method of microscopy. However, a consistent pattern could not be seen in the structure of this fiber formation. Some of the gels contained a more “web-like” pattern (Fig 3a), while others had a striated pattern to their fibers (Fig 4b). Similarly, previous studies that have imaged collagen in tumors using this method did not appear to show a consistent pattern in the alignment of fibers *in vivo* [14,15].

Fiber Density and Overall Fiber Formation:

Fiber density refers to the concentration of fibers seen in a given field of view. With the naked eye, it appeared that this density increased with increasing concentration of gel. However, quantification of these images showed very little difference in percent of collagen positive areas between the 5 mg/mL and 7 mg/mL collagen gels (Fig 7). The

first set of images obtained using this method of microscopy showed fibers that appeared to be clustered in certain areas of the sample. However, in subsequent batches of samples, it could be seen that the center of the gel showed much greater fiber density. This could be seen visually because the images taken at the center of the gel dot were much brighter, irrespective of the laser intensity used (Fig 3b and Fig 4b). It appeared that the density of fibers decreased as field of view was moved further away from the center. However, quantification of the images indicated that there were very little differences in fiber density between images taken at the center of the gel and those taken closer to the outer edges (Fig 8). Only the 7 mg/mL concentration gels appeared to show a slightly lower percent of collagen positive area for the images taken at the outer edges of the gel (Fig 7b).

Diffusion Experiment

This experimental setup showed that the 3kDa dextran diffused out of the collagen the fastest, while the 2MDa dextran took much longer to diffuse. Although the experiment was run for 18 hours, less than 50% of the 2MDa diffused from the gel. Due to the size-dependent nature of diffusion, it was expected that the smaller dextrans would diffuse much faster than the larger dextrans. These experimental results did indeed align with this expectation. Given that all other parameters were kept constant for each molecule and gel combination tested, the differences in diffusion coefficients explain the variations seen in the diffusion times for each molecule. This observation was further validated by the calculation of the diffusion coefficients for the dextrans and the literature values found in previous studies. The 3kDa had the lowest diffusion coefficient, while the 2MDa Tritc had a much greater value (Tables 3 and 4). It should be pointed out that the literature values obtained were based on gels of a much greater concentration than ones used in this study. However, because the gels used in this study were of a much lower concentration, the calculated values were much lower. Overall, the relationship between size, diffusion time and diffusion coefficient remained the same: Diffusion coefficient

increased with increasing size of molecule and, thereby, resulting in slower diffusion times.

Although the diffusion experiment validated the expected outcome for the diffusion of dextrans through these gels, it also served as a proof-of-concept for the underlying purpose for the use of the collagen gels. These results corroborated the notion that these collagen gels do indeed allow for movement of particles through the fiber network. This was evident in the diffusion of the dextrans from inside the gel into the PBS solution surrounding the gel. Therefore, these gels can be used in further testing of nanoparticle drug delivery and in the future development of a microfluidic testing device that would contain a collagen matrix to mimic the tumor environment.

It is important to note that the diffusion experiment was conducted using only one concentration of gel, which was a concentration of 1.5 mg/mL. In order to understand the effects of the collagen on the movement of these particles, further testing would need to be conducted using higher concentrations of gels. It is expected that higher concentrations of gels would correspond to lower diffusion times for each molecule between the concentrations tested. This effect would stem primarily from the presence of more fibers in the gels, thereby, hindering the free movement of the dextrans through the gels.

CHAPTER 6

CONCLUSION

The primary goal of this study was to lay the groundwork for a collagen-based model for NP drug testing. The use of collagen gels served as the basis for this work. After the creation of gels, 2-photon microscopy was utilized to confirm and analyze fiber formation in these gels. General patterns were seen in the fiber structure and density of the gels created. Furthermore, this set of experiments validated the use of microscopy to visualize collagen gels, as opposed to traditional methods that involve the use of dyes. In addition, the diffusion experiment served as a proof-of-concept for future work that will be done using these collagen gels as a testing model for drug delivery. Because the results aligned with the expected diffusion patterns, this set of experiments indicated that these gels could be used to study how particles move through the pores, a feature that can be extended to what is seen *in vivo* in tumor tissues.

Future work stemming from this work will require further analysis of the collagen gels. For example, it will be important to study the mechanical properties of the gels, including the elasticity of the collagen. This will ensure that the gels are indeed similar to what is seen in tumors, especially because it is desirable for this model to simulate *in vivo* conditions. Extensions of the diffusion experiment will include testing collagen gels of varying concentrations. In addition, it will be essential to determine the appropriate concentration of gel to be used and use only that specific concentration for subsequent experimentation. Similarly, this concentration would need to be close to values seen in actual tumors.

REFERENCES

- [1] CDC. (2015). World Cancer Day. Retrieved from <http://www.cdc.gov/cancer/dcpc/resources/features/worldcancerday/>
- [2] Matsumura, Y. and Maeda, H. (1986). A new concept for macromolecular therapeutics in cancer-chemotherapy – mechanism of tumoritropic accumulation of proteins and the antitumor agent SMANCS. *Cancer Research*, 46(12), 6387-6392.
- [3] Wong, C., Stylianopoulos, T., Cui, J. A., Martin, J., Chauhan, V. P., Jiang, W., Fukumura, D. (2011). Multistage nanoparticle delivery system for deep penetration into tumor tissue. *Proceedings of the National Academy of Sciences of the United States of America*, 108(6), 2426-2431.
- [4] von Maltzahn, G., Park, J. H., Lin, K. Y., Singh, N., Schwoppe, C., Mesters, R., Bhatia, S. N. (2011). Nanoparticles that communicate in vivo to amplify tumour targeting. *Nature Materials*, 10(7), 545-552. doi:10.1038/nmat3049
- [5] Kwak, B., Ozcelikkale, A., Shin, C. S., Park, K., & Han, B. (2014). Simulation of complex transport of nanoparticles around a tumor using tumor-microenvironment-on-chip. *Journal of Controlled Release*, 194, 157-167.
- [6] Fang, M., Yuan, J.P., Peng, C.W., & Li, Y. (2014). Collagen as a double-edged sword in tumor progression. *Tumor Biology*, 35(4), 2871-2882.
- [7] Ryan, G. M., Kaminskas, L. M., & Porter, C. J. H. (2014). Nano-chemotherapeutics: Maximising lymphatic drug exposure to improve the treatment of lymph-metastatic cancers. *Journal of Controlled Release*, 193, 241-256.
- [8] Maeda, H., Wu, J., Sawa, T., Matsumura, Y. & Hori, K. (2000). Tumor vascular permeability and the EPR effect in macromolecular therapeutics. *Journal of Controlled Release*, 65(1-2), 271-284.
- [9] Sun, T.M., Zhang, Y.S., Pang, B., Hyun, D.C., Yang, M.X. & Xia, Y.N. (2014). Engineered Nanoparticles for drug delivery in cancer therapy. *Angewandte Chemie – International Edition*, 53(46), 12320-12364.
- [10] Ruan, S. B., Cao, X., Cun, X. L., Hu, G. L., Zhou, Y., Zhang, Y. J., Gao, H. L. (2015). Matrix metalloproteinase-sensitive size-shrinkable nanoparticles for deep tumor penetration and pH triggered doxorubicin release. *Biomaterials*, 60, 100-110.
- [11] Ramanujan, S., Pluen, A., McKee, T., Brown, E.B., Yves, B. & Jain, R. (2002). Diffusion and convection in collagen gels: implications for transport in the tumor interstitium. *Journal of Biophysics*, 8(3), 1650-1660.
- [12] Choi, J.J., Wang, S., Tung, Y.S., Morrison, B. & Konofagou, E.E. (2011). Molecules of various pharmacologically-relevant sizes can cross the ultrasound-induced blood brain barrier opening in vivo. *Journal of Ultrasound Medical Biology*, 36(1), 58-67.
- [13] TdB Consultancy (2010). TRITC-Dextran. Retrieved from http://tdbcons.com/images/pdf/tritc_dextran.pdf
- [14] Brown, E., McKee, T., diTomaso, E., Puen, A., Boucher, Y., Jain, R.K. (2003). Dynamic imaging of collagen and its modulation in tumors in vivo using second-harmonic imaging. *Nature Medicine*, 9, 796-800

- [15] Walsh, A.J., Cook, R.S., Lee, J.H., Arteaga, C.L., Skala, M.C. (2015). Collagen density and alignment in responsive resistant trastuzumab-treated breast cancer xenografts. *Journal of Biomedical Optics*, 20(2), 0260041-8.